J Solid State Electrochem (2007) 11:469–477
DOI 10.1007/s10008-006-0175-2

ORIGINAL PAPER

Oxygen stoichiometry, unit cell volume, and thermodynamic quantities of perovskite-type oxides

Egle Girdauskaite · Helmut Ullmann · Mahmoud Al Daroukh · Vladimir Vashook · Martin Bülow · Ulrich Guth

Received: 11 April 2006 / Revised: 24 April 2006 / Accepted: 10 May 2006 / Published online: 23 June 2006

Abstract Perovskite-type oxides $A_{1-a}A'_aB_{1-b}B'_bO_{3-x}$ with A, A′=La, Ba, Sr; B, B′=Mn, Fe, Co were investigated by means of thermal analysis, solid electrolyte cells, and X-ray diffraction. Partial molar thermodynamic quantities are determined and their relations with O/M stoichiometry, unit cell volume, and phase stability were studied. The absolute values of partial molar enthalpies of perovskite-type oxides increase with increasing O/M stoichiometries and with decreasing unit cell volumes of the cubic perovskite-type structure, corresponding to higher chemical stabilities. The substitution of Ba for La, Ba for Sr, Co for Fe, and Fe for Mn lead to increase in unit cell volumes and decrease in absolute values of ΔH^0. The ΔH^0 values of the cobaltites/ferrites range from −33.5 kJ/mol for $SrCo_{0.8}Fe_{0.2}O_{3-x}$ to −72.5 kJ/mol for $La_{0.2}Sr_{0.8}Co_{0.6}Fe_{0.4}O_{3-x}$, and of the manganates up to −132 kJ/mol for $Ca_{0.5}Sr_{0.5}Mn_{0.8}Fe_{0.2}O_{3-x}$.

Keywords Perovskite-type oxides · O/M stoichiometry · Thermodynamic data · Lattice parameters

Introduction

Oxide ceramic materials with high oxygen transport are of interest as oxygen permeation membranes and oxygen-storage materials with regard to various applications. Mixed ionic–electronic conductors of the perovskite-type structure with high oxide ion and electron transport [1, 2] are used in solid oxide fuel cells, in oxygen membrane reactors, and in ceramic oxygen sorbents for cyclic absorption–desorption reactions. These applications require temperatures as high as 973 to 1,173 K. The applicability of the above-mentioned processes had been demonstrated at laboratory scale by several research groups as recently reviewed by [3].

The development of improved oxide materials with high oxygen transport plays a key role in technical execution of those advanced technologies. In addition to high oxygen fluxes, the materials need to exhibit sufficient chemical and structural stabilities as well as favorable thermo-mechanical resistance. Oxygen diffusion and surface-exchange rates of the oxide ceramic materials should be high. Of interest are, first of all, the thermodynamics and kinetics of reactions between oxygen from the gaseous environment and the oxide material. At present, many empirical results on the investigation of oxide materials of practical interest are available, but there is a lack of reliable fundamental data. In this report, the methods of investigation and results on thermodynamic data of oxygen-oxide solid-solution reactions are presented and correlated with parameters of the crystal lattice.

E. Girdauskaite · H. Ullmann (✉) · M. Al Daroukh · V. Vashook · U. Guth
Institut für Physikal. Chemie und Elektrochemie,
Technische Universität Dresden,
D-01062 Dresden, Germany
e-mail: Helmut.Ullmann@chemie.tu-dresden.de

M. Bülow
BOC PGS Technology,
100 Mountain Avenue,
Murray Hill, NJ 07974, USA

Fundamental characteristics of mixed conducting oxides

Crystal and defect structures

Oxides for high oxygen transport should exhibit high oxide-ion diffusion and high surface-exchange rates. A certain appropriate crystal structure and defect structure are major prerequisites for the transport of the relatively large oxide ions. The crystal structure is characterized by cor-

responding geometrical relations, by a predominant ionic type of bonding and moderate oxidation numbers of the cations. The coordination number of oxide ions towards cations should be high to enable moderate bonding forces and interchangeable oxygen sites. Fluorite and perovskite types of structure meet these requirements preferentially.

Besides the type of crystal structure, the defect structure of the lattice is of interest for transport characteristics. The oxide ions are transported through lattice defects, mostly by a vacancy mechanism, rarely by an oxygen interstitial mechanism. The introduction of isovalent cations of different ionic radii generates mechanical tension within the crystal lattice. Heterovalent cations additionally generate acceptor- or donor-type electrical charge defects. The vacancies in the oxygen sublattice are formed both by heterovalent cationic substitution and by partial reduction of transition-metal cations. The substitution of cations changes the O/M stoichiometry and/or the A/B-site stoichiometry. The overall formula of a substituted perovskite-type compound of oxygen vacancy-type defect structure, which is of main interest, is written as $A_{1-a}A'_aB_{1-b}B'_bO_{3-x}V^{\bullet\bullet}_{O,x}$ (metal cations M=A+A′+B+B′; A, A′=rare-earth or earth-alkaline; B, B′=transition metal ion of the fourth row of the periodic system of elements, $V^{\bullet\bullet}_{O}$ =oxygen vacancy).

Up to a certain concentration, oxygen vacancies within the oxygen sublattice of perovskite-type structures are randomly distributed. Increasing concentrations of ionic and electronic defects in the crystal cause an increase in the transport rate of oxide ions through oxygen vacancies of the lattice and a simultaneous decrease in the chemical stability of the oxide, which simultaneously weakens the thermo-mechanical stability of the oxide ceramic materials. At very high concentrations of defects, an increase in ordering with formation of clusters up to formation of new phases is observed and accompanied by a decrease in mobility of the oxide ions.

Chemical composition

The enhancement of oxygen transport in perovskite-type oxides by increasing earth alkaline (A′) substitution is a general trend observed in published investigations, which results in acceptor-doped perovskite-type oxides. The increasing ionic radii of A′ (Ba > Sr > Ca) and decreasing thermodynamic stabilities of the B-site metal oxides (Mn > Fe > Co) enhance the oxide-ion transport due to lowered chemical bonding to the oxide ions, increased lattice parameters, and vacancy concentrations. The electronic and ionic transport rates increase with increasing contents of Sr and Co. $SrCoO_{3-x}$ shows one of the highest levels of oxide-ionic transport, but its cubic perovskite-type phase only exists at temperatures above 1,238 K [4]. Thus, $SrCo_{0.8}Fe_{0.2}O_{3-x}$ was the starting oxide to search for stable materials with high oxygen transport. To extend the stability limits of the perovskite phase towards lower oxygen pressures and lower temperatures, additional substitution on A and B sites was required [5], which, in its turn, led to the intensively investigated $La_{1-a}Sr_aCo_{1-b}Fe_bO_{3-x}$ mixed oxides [1, 6–9]. The introduction of Ba at the La sites results in enhanced oxygen transport rate that is explained by the occurrence of higher values of the lattice parameter [10]. To increase the reduction stability, a complete renunciation of Co is proposed [11, 12].

Oxygen exchange capacity and O/M stoichiometry

The amount x of reversibly exchangeable oxygen of a perovskite-type oxide $A_{1-a}A'_aB_{1-b}B'_bO_{3-x}$ is a function of temperature and oxygen activity gradient between the surface and the center of the crystallite. The oxygen sublattice of the perovskite structure is completely occupied at an O/M stoichiometry of 3.0. Oxygen excess at high oxygen partial pressure pO_2 as a result of cation vacancy formation is observed exclusively in manganates [13]. Complete occupation of the oxygen sublattice is reached at higher pO_2 in the gas phase. The required pressure increases in accordance with the sequence Cr < Mn < Fe < Co < Ni that is caused by the preferred oxidation states of the B cations. At decreasing pO_2, each of the perovskite-type oxides approaches to a level of relative independence of the O/M stoichiometry of pO_2 characterized by the average oxidation state 3+ of the B cations, corresponding to $B^{\bullet}$=B′ [14]. At this level, O/M becomes equal to $(3-a/2)$. For ferrites and cobaltites, this point is reached at pO_2 values near or below 1 Pa in argon. In Fig. 1, these relations are given schematically.

Thermo-mechanical properties

The thermo-mechanical properties of metal oxides are influenced by thermal expansion due to the electrostatic attraction forces and thermal oscillations of the ions within the crystal lattice. The lattice energy diminishes with decreasing positive and negative electric charges within the lattice. Thus, an empirical correlation between vacancy concentration, oxide ionic transport, and thermal expansion coefficients of perovskite-type oxides is expected. The concentration of vacancies is simultaneously reflected by the unit cell volumes of the crystals. Therefore, correlations between thermodynamic and transport properties with thermal expansion and lattice parameters of oxides are expected. In case of an oxide membrane between two gases of different oxygen partial pressure and due to O/M gradients through the membrane, the lattice constants and, consequently, the thermal expansion increases from higher to lower O/M ratios [15]. High values and high gradients of

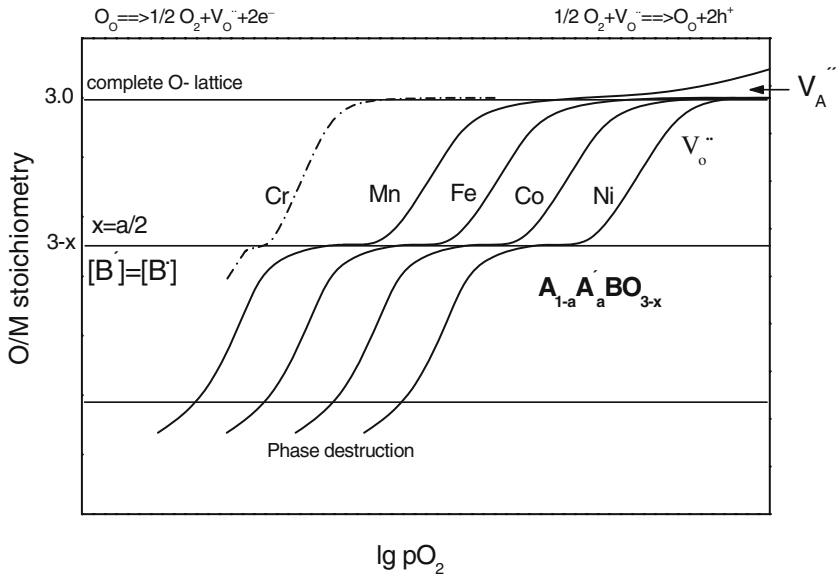

Fig. 1 Schematic diagram of the oxygen-to-metal (O/M) stoichiometry ($3-x$) vs log pO_2 for perovskite-type oxides $A_{1-a}A'_aB_{1-b}B'_bO_{3-x}$. $V_O^{\bullet\bullet}$ oxide ion vacancy region. V_A'' cation vacancy region, assuming A site is occupied by A^{2+}

thermal expansion coefficients of the ceramic materials result in thermo-mechanical properties that would be insufficient for practical utilization. There are attempts to minimize thermal expansion and mechanical stresses by formation of composites with two or more oxide phases or of ceramic–metal composites (cermets) [3].

Experimental

Preparation and structural characterization of the oxide samples

The starting compounds were $SrCO_3$, $BaCO_3$, La_2O_3, CeO_2, Co_3O_4, Fe_3O_4, and Mn_2O_3 (p.a.). The powders of those compounds were initially ground, mixed, and allowed to react at 1,000 °C in air, than crashed, ground, and heated in air for 10 h at a temperature required for perovskite-phase formation, followed by cooling the products down to room temperature with a rate of 5 K/min. The ceramic pellets were produced by pressing the powders and sintering in air at a temperature of 323 to 373 K higher than the temperature of powder annealing. The formation of the perovskite-phase and the lattice parameters were determined by X-ray diffraction (XRD) measurements. XRD patterns were obtained by means of a Siemens D-5000 equipment with monochromatic CuK_α radiation.

The following gases of different oxygen partial pressures were used in the experiments: oxygen, air, and Ar/O_2 gas mixture with 1, 400, and 2,000 Pa O_2; these gases were prepared by mixing or solid electrolytic pumping oxygen into commercial argon. Ar/H_2,H_2O mixtures were prepared by pumping oxygen into Ar/H_2.

Oxygen exchange measurements

Oxygen uptake and release was measured in the temperature range of 673 to 1,173 K by a micro-thermo balance (Fig. 2). In the upper section of a quartz tube (30-mm diameter), a quartz spring was arranged to which a porous ceramic sample was fixed by means of a platinum wire. The sample was placed in the heating zone (T range 673 to 1,173 K). The extension of the spring due to oxygen uptake was optically read by a cathetometer with a sensitivity of 0.3 mm/mg. The calibration of the spring balance was performed at defined gas flows and temperatures. By shifting of the sample within the furnace as a result of different sample weights (370 to 390 mg) and oxygen uptake/release of the oxides, a temperature error of maximal 10 K may arise. A gas of controlled oxygen partial pressure flows with a steady flow rate of about 5 l/h through the thermo balance.

For measurements of oxygen in argon/oxygen mixtures in higher concentration ranges, an amperometric lambda sensor (Bosch, Germany) was used. The sensor was placed in the gas stream at the exit of the thermo balance. Within the range of oxygen contents of air to argon/O_2, the diffusion-limited current of the sensor at constant voltage of 600 mV depends linearly on the oxygen concentration in the gas stream.

Chemical stability measurements and determination of the O/M stoichiometry

The chemical stabilities of the oxides were investigated by annealing the powder samples in a quartz container during heating in argon/O_2 and argon/H_2/H_2O gas. The oxygen

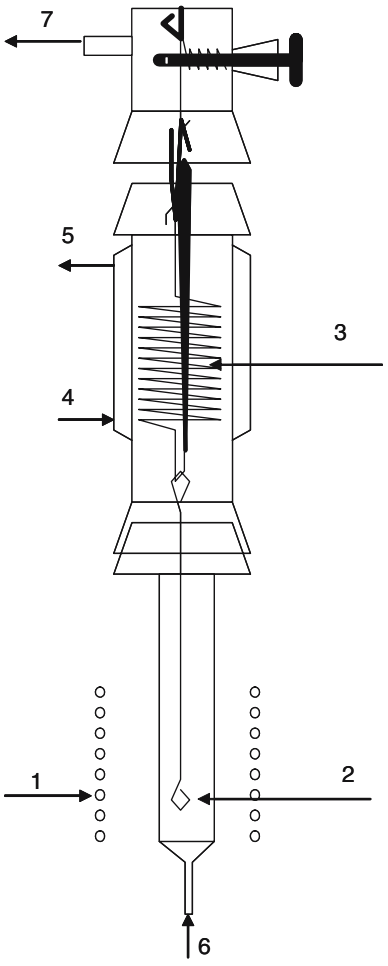

Fig. 2 Micro-thermo balance with quartz spring for measurements of high-T oxygen-sorption isotherms. *1*, heater, *2* sample holder, *3* quartz spring, *4* and *5* thermostat with water inlet and outlet, *6* and *7* reaction gas inlet and outlet

partial pressure of the reaction gas was measured potentiometrically by a zirconia solid-electrolyte arrangement (Fig. 3) with two cells placed before and after the reaction furnace [16]. XRD patterns (12-h measurement time) of both initial and reduced sample powders indicate the structure stability of samples in gases of different oxygen partial pressures.

The O/M relations ($3-x$) of the manganites in the air-prepared state (at the temperature of phase formation and 5 K/min cooling down to room temperature) can be assumed to be nearly 3.0 [15]. The O/M stoichiometries of the cobaltites/ferrites are only accessible by analytic investigation. The O/M stoichiometries were determined by solid electrolyte measurements as oxygen amount χ released between the air-prepared state and the argon/1 Pa O_2-equilibrated state ($x=a/2$ in Fig. 1).

Oxygen uptake and release experiments were carried out by thermogravimetric measurements during heating up and cooling down at a rate of 5 K/min in an atmosphere of constant pO_2. As starting point, the equilibrium of the oxides with 1 atm O_2 at 673 K was chosen. In the first run, the oxygen uptake of some samples between 1 atm O_2/673 K and room temperature may differ due to uncontrolled adsorption of other gaseous species such as water vapor and carbon dioxide. In these cases, sorption experiments are repeated up to constant values.

Results and discussion

O/M stoichiometry and chemical stability

The results of measurement of the O/M relations are given in Table 1. All cobaltites/ferrites, exclusively the $La_{0.2}Sr_{0.8}Co_{0.6}Fe_{0.4}O_{3-x}$, in the air-prepared state show considerable deviations from the stoichiometry 3.0, indicating, thus, incompletely occupied oxide lattices. Other authors at total reduction and thermogravimetric analysis on La/Sr–cobaltites [17], La/Sr–ferrites [18], and iodometric titration on La/Sr–cobaltites/ferrites [19] generally found completely occupied oxide lattices. The reason for the incomplete occupation in our compositions may be the total occupation of the A site by A^{2+} cations. The released contents of oxygen from different compositions in pure oxygen atmosphere are given in Fig. 4. The results indicate that the exchange stopped completely below 473 K and for manganates even at 673 K. The frozen O/M stoichiometries of the as-prepared powders will not only depend on cationic composition but even on surface/volume ratio, on gaseous dynamics during cooling, and on the overall history of the sample as well.

XRD patterns demonstrate the chemical and phase stability after annealing at 1,073 K in argon/1 Pa O_2. In argon/H_2/H_2O mixtures with $pO_2=10^{-9}$ Pa, the cobaltites/ferrites are decomposed. The manganites/ferrites show only traces of phase destruction (example in Fig. 5a), the main

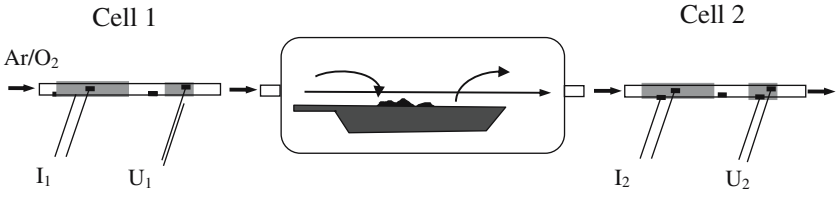

Fig. 3 Solid-electrolyte arrangement for oxide/oxygen equilibrium measurements. Cells 1 and 2 with the voltages U_1 and U_2

Table 1 O/M stoichiometries (3−x) of perovskite-type oxides after air preparation and slow cooling (5 K/min) to room temperature

Composition	Abbreviations	Preparation temperature (K)	3−x (air)
$Ba_{0.5}Sr_{0.5}Co_{0.8}Fe_{0.2}O_{3-x}$	BSCF5582	1,373	2.75
$Ba_{0.5}Sr_{0.5}Co_{0.6}Fe_{0.4}O_{3-x}$	BSCF5564	1,373	2.74
$Ba_{0.3}Sr_{0.7}Co_{0.8}Fe_{0.2}O_{3-x}$	BSCF3782	1,373	2.81
$La_{0.2}Sr_{0.8}Co_{0.6}Fe_{0.4}O_{3-x}$	LSCF2864	1,373	2.95
$Ca_{0.5}Sr_{0.5}Mn_{0.9}Fe_{0.1}O_{3-x}$	CaSMF5591	1,473	(3.0)[a]
$Ca_{0.5}Sr_{0.5}Mn_{0.8}Fe_{0.2}O_{3-x}$	CaSMF5582	1,473	(3.0)[a]
$Ca_{0.5}Sr_{0.5}Mn_{0.5}Fe_{0.5}O_{3-x}$	CaSMF5555	1,473	(3.0)[a]
$Ca_{0.2}Sr_{0.7}Mn_{0.8}Fe_{0.2}O_{3-x}$	CaSMF2782	1,473	(3.0)[a]

[a]Assumed after the results in [15]

peak of the perovskite phase being shifted to higher lattice constants with decreasing pO_2. After $Ar/H_2/H_2O$ annealing, the cubic modification was found to have changed into a hexagonal one (Fig. 5b).

Oxygen-oxide reactions: enthalpies and entropies

Depending on the position within the lg pO_2 vs $1/T$ phase diagram, three different reaction types of the metal oxide/oxygen reaction are observed. The examples of the various reaction types in the system Sr–Co–O were described earlier [20]. At the phase boundary of Co_3O_4/CoO, the reaction results into a structural change to form a new compound accompanied by nonlinear changes in physico-chemical properties [reaction type (1)]. Oxygen release started at the temperature of phase transition to CoO. In reaction (1), the crystal structure transforms completely from ferrite type to NaCl type. The observed absolute values of the reaction enthalpy and entropy are the highest among the three reaction types. Between the phase boundaries, the reaction of a stable perovskite-type oxide, e.g., $Sr_{0.965}Ce_{0.035}CoO_{2.535+n}$ [21], with δ oxygen leads to a solid solution with changing O/M stoichiometry and changing concentration of lattice defects, whereas the structure type remains unchanged [reaction type (2)]. The solid-solution reaction is characterized by the lowest values of enthalpy in this row. The growing defect concentrations may cause an ordering or cluster formation as a preliminary stage of phase transition [reaction type (3)], as investigated for $SrCoO_{2.5}$ by [22]. Reaction (3) is characterized by a rhombohedral-to-pseudocubic reorientation within the perovskite-related structure type, which is connected with moderate values of reaction enthalpy and entropy. The absolute values of ΔH^0 decrease with decreasing amount δ of exchanged oxygen.

In this work, the partial molar quantities of further perovskite-type oxides within the range of solid-solution reaction are determined. The oxygen exchange δ related to the 673 K/1 atm O_2 equilibrium as starting point is measured during heating and cooling in the form of isobars. The isotherms (Fig. 6a) are constructed therefrom. For each isostoichiometric composition (δ=constant), a ln pO_2 vs $1/T$ curve exists (Fig. 6b). Partial molar reaction enthalpies and entropies are obtained from plots ln (pO_2) vs $1/T$, i.e., from slopes and intercepts with the vertical axis,

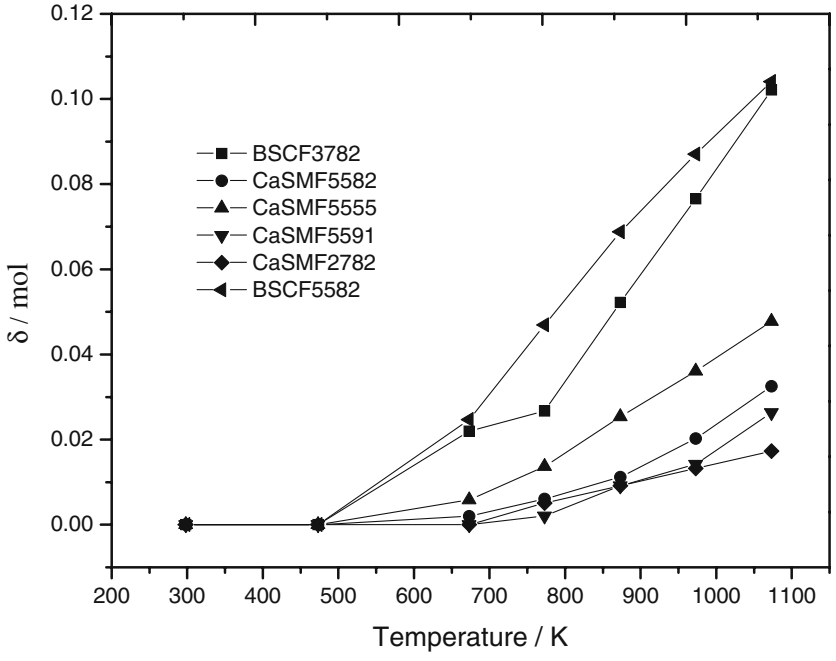

Fig. 4 Absorption/desorption of oxygen amounts δ (mol) from perovskite-type oxides at 1 atm O_2 between the compositions at room temperature and 1,073 K measured by thermo balance

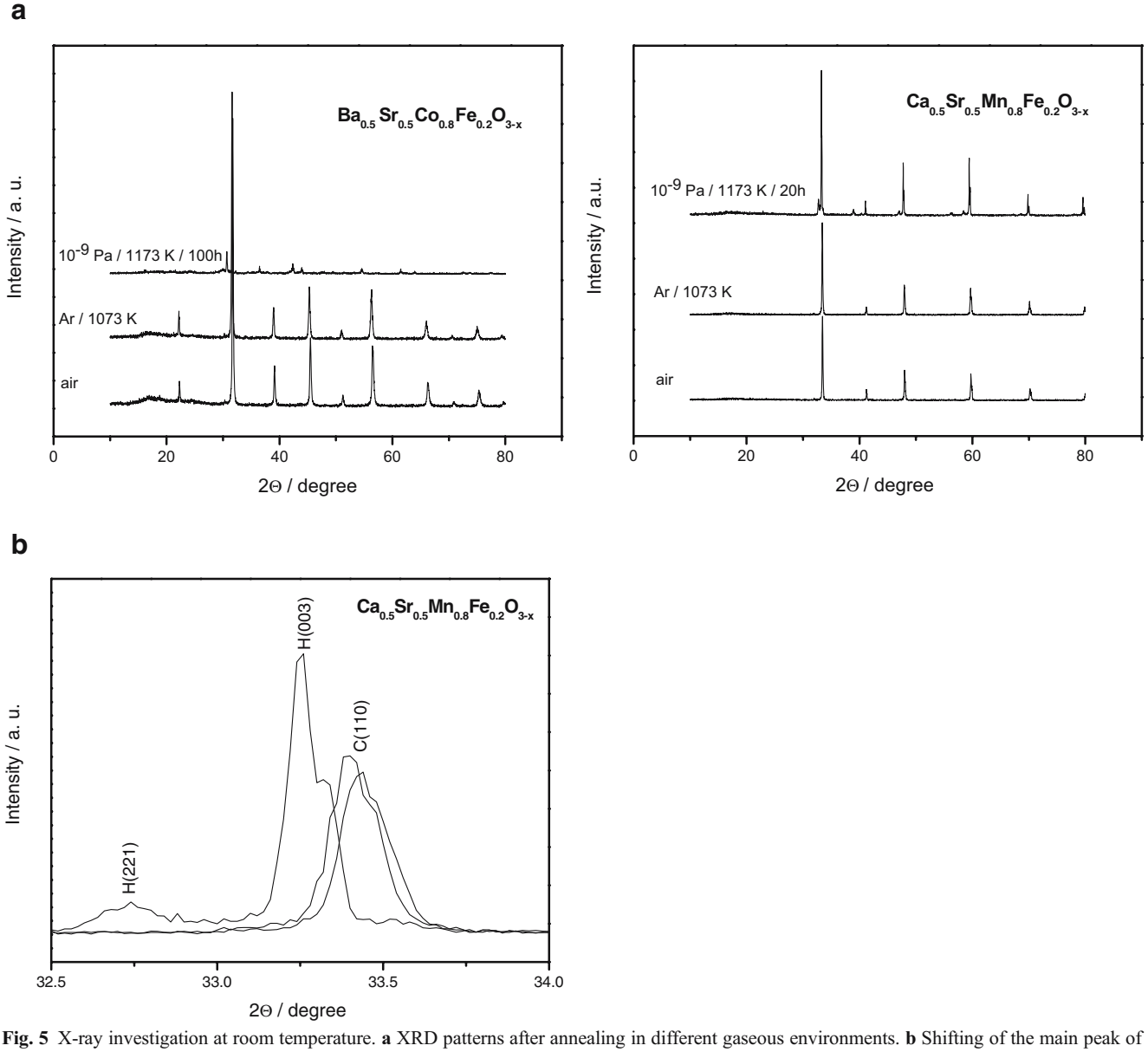

Fig. 5 X-ray investigation at room temperature. **a** XRD patterns after annealing in different gaseous environments. **b** Shifting of the main peak of the cubic perovskite-type structure C(110) to higher theta values by oxygen loss. H(003) corresponds to the hexagonal structure type

respectively. The calculations of changes in enthalpy and entropy follow the formalism for the reaction shown. For understanding: The O/M stoichiometry ($3-x$) at the starting point of any exchange experiment for an actual composition is quantified as $3-(a/2)+n$ in the oxygen-richer state and as $3-a/2+n-\delta$ in the oxygen-poorer state.

$$Ba_{0.3}Sr_{0.7}Co_{0.8}Fe_{0.2}O_{2.5+n-\delta} + \delta\ /2O_2 \Leftrightarrow Ba_{0.3}Sr_{0.7}Co_{0.8}Fe_{0.2}O_{2.5+n}$$

with the equilibrium constant

$$K_a' = (pO_2)^{-\delta/2}$$

Related to the reaction with 1 mol of atomic oxygen:

$$\Delta G^0 = -RT \ln K_a = -RT \ln (pO_2)^{1/2}$$

$$\Delta G^0 = \Delta H^0 - TS^0$$

$$\ln pO_2 = \frac{-2\Delta H^0}{R} \cdot \frac{1}{T} + \frac{2S^0}{R}$$

In a simplified version, this corresponds to the reaction of free oxygen sites (vacancies) with gaseous oxygen:

$$V_0^{\bullet\bullet} + 1/2O_2 \Leftrightarrow O_o^x$$

The differences in values of thermodynamic quantities are caused by different activities of oxygen vacancies in the

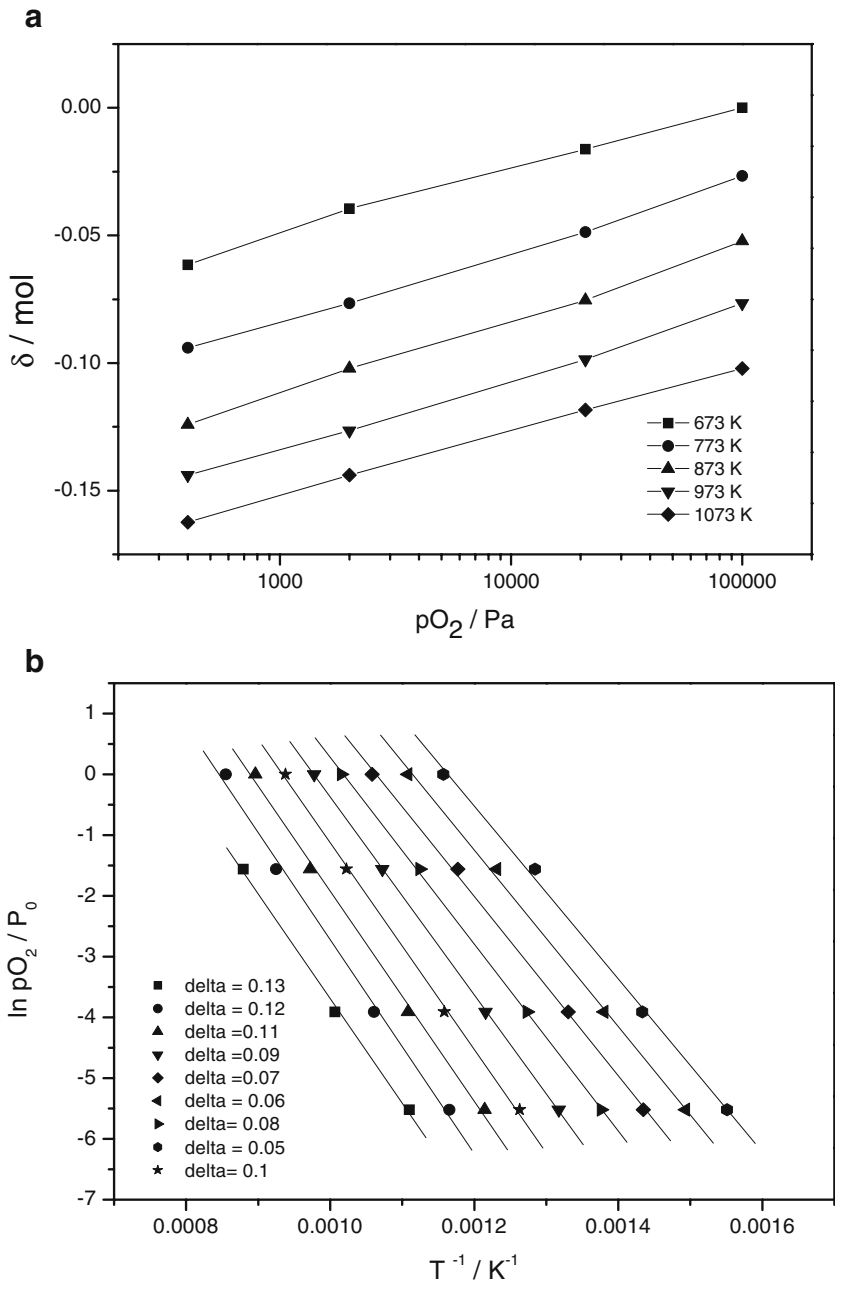

Fig. 6 Oxygen absorption and desorption of the reaction of $Ba_{0.3}Sr_{0.7}Co_{0.8}Fe_{0.2}O_{2.5+n-\delta} + \delta/2\ O_2 \Leftrightarrow Ba_{0.3}Sr_{0.7}Co_{0.8}Fe_{0.2}O_{2.5+n}$. **a** Isotherms of the reaction. **b** ln pO_2–$1/T$ diagram

actual solid solution (composition and structure of the oxide).

The tabulated partial thermodynamic quantities (Table 2) are that for the lowest δ values, i.e., near the compositions that correspond to 673 K/1 atm O_2 equilibrium. The absolute values of ΔH^0 are in accordance with the δ values. The oxides with the highest oxygen exchange capacities in Fig. 4 have the lowest ΔH^0 values that indicate lowest thermodynamic stabilities of the oxides. The manganates have generally higher ΔH^0 values (except that of $Sr_{0.5}Ca_{0.5}Mn_{0.5}Fe_{0.5}O_{3-x}$) and lower unit cell volumes. For each composition (excluding the behavior of $Sr_{0.5}Ca_{0.5}Mn_{0.5}Fe_{0.5}O_{3-x}$), the enthalpy values increase with decreasing δ, which corresponds to increasing stability of the oxide (Fig. 7a). This tendency agrees with the observations of [17, 19].

The correlation of the unit cell volumes with the thermodynamic data must be seen qualitatively because the former were measured at room temperature in air. In $Ba_{1-a}Sr_aCo_{1-b}Fe_bO_{3-x}$, the unit cell volumes increase and the absolute values of ΔH^0 decrease with decreasing Sr content and with substitution of La by Ba. At constant Ba/Sr ratio,

Table 2 Unit cell volumes and thermodynamic quantities of perovskite-type oxides

Compositions investigated in this work	Structure (air/Ar)	Unit cell volume ($Å^3$)air/argon	$-\Delta H^0$ (kJ/mol)	S^0 (J/mol K)
$SrCo_{0.8}Fe_{0.2}O_{3-x}$	Cub/orth	57.7/60.8	33.5	36
$Sr_{0.965}Ce_{0.035}CoO_{3-x}$	Tetr/non per	1,378.4	54.1	58
$La_{0.2}Sr_{0.8}Co_{0.6}Fe_{0.4}O_{3-x}$	Hex/hex	170.3/172.5	72.5	87
$Ba_{0.5}Sr_{0.5}Co_{0.8}Fe_{0.2}O_{3-x}$	Cub/cub	63.4/64.1	38.0	34
$Ba_{0.5}Sr_{0.5}Co_{0.6}Fe_{0.4}O_{3-x}$	Cub/cub	62.9/63.7	51.0	56
$Ba_{0.3}Sr_{0.7}Co_{0.8}Fe_{0.2}O_{3-x}$	Cub/cub	61.2/61.8	59.2	69
$Ca_{0.5}Sr_{0.5}Mn_{0.9}Fe_{0.1}O_{3-x}$	Cub/cub	54.2/54.5	104.8	107
$Ca_{0.5}Sr_{0.5}Mn_{0.5}Fe_{0.5}O_{3-x}$	Cub/cub	55.4/55.8	48.0	58
$Ca_{0.5}Sr_{0.5}Mn_{0.8}Fe_{0.2}O_{3-x}$	Cub/cub	54.4/54.6	132.0	75
$Ca_{0.2}Sr_{0.7}Mn_{0.8}Fe_{0.2}O_{3-x}$	Hex/orth	238.0/304	63.6	85

ΔH^0 decreases, and the unit cell volume increases with increasing Co content. The more stable manganates show highest absolute values of ΔH^0 and generally lower unit cell volumes. It should, however, be kept in mind that only compositions of identical structural modifications can be compared. Further investigation is required to clear up this correlation.

Mizusaki et al. [17] investigated a series of La,Sr cobaltites, and they found that the absolute values of ΔH^0 decrease with increasing Sr content. The ΔH^0 value of

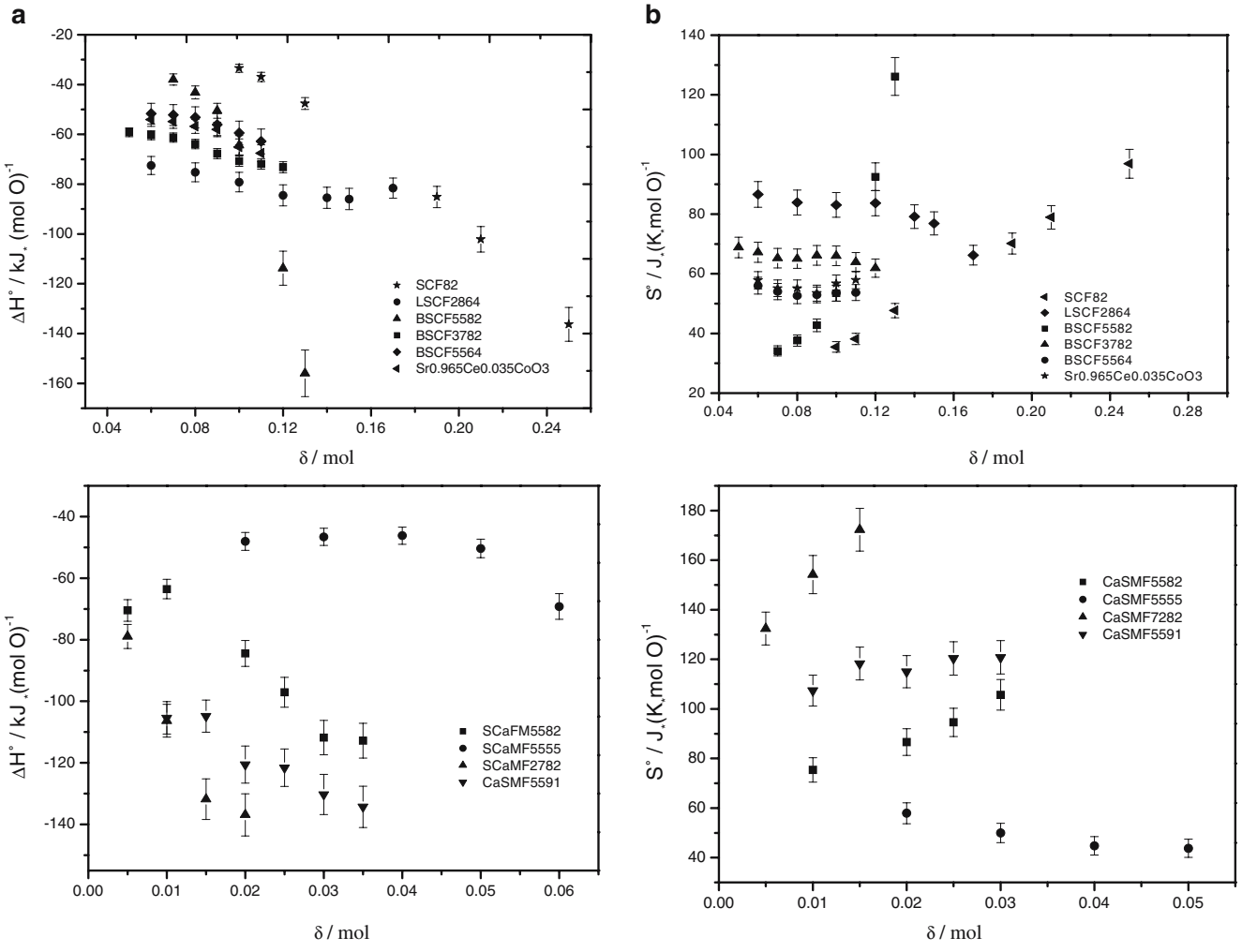

Fig. 7 Partial molar thermodynamic quantities of perovskite-type oxides as a function of changes δ (mol) of the O/M stoichiometry. **a** Enthalpy ΔH^0. **b** Entropy S^0

$La_{0.3}Sr_{0.7}CoO_{3-x}$ (75.5 kJ/mol) is about that of $La_{0.2}Sr_{0.8}Co_{0.6}Fe_{0.4}O_{3-x}$ (−72.5 kJ/mol) found in our work.

The entropy values (Fig. 7b) of the $Ba_{1-a}Sr_aCo_{1-b}Fe_bO_{3-x}$ do not show clear tendencies vs δ. The S^0 values of the manganates decrease with decreasing δ, what agrees with the observations of [17, 19] explained by the decrease of configurational entropy of oxygen in the oxide.

Conclusions

The investigations performed on perovskite-type oxides $A_{1-a}A'_aB_{1-b}B'_bO_{3-x}$ (A, A′=La, Ba, Sr; B, B′=Mn, Fe, Co) demonstrate relationships between O/M stoichiometry, unit cell volume, phase stability, and thermodynamic quantities. The absolute values of partial molar enthalpies of perovskite-type oxides increase with increasing O/M stoichiometries and with decreasing unit cell volumes of the cubic perovskite structures corresponding to higher chemical stabilities. Thus, the substitutions of Ba for La, Ba for Sr, Co for Fe, and Fe for Mn lead to an increase in unit cell volumes and to a decrease in absolute values of ΔH^0. Further investigation is projected for the correlation of the results with thermal expansion behavior.

References

1. Teraoka Y, Zhang HM, Furukawa S, Yamazoe M (1985) Chem Lett 1743
2. Teraoka Y, Nobunaga T, Yamazoe M (1988) Chem Lett 503
3. Ullmann H, Guth U, Vashook VV, Bülow M, Burckhardt W, Götz R (2004) Ceramic oxides with high oxygen transport. In: Pandalai SG (ed) Recent research developments in solid state ionics 2. Transworld Research Network Kerala/India 347:366
4. Vashook VV, Zinkevich MV, Ullmann H, Paulsen J, Trofimenko N, Teske K (1997) Solid State Ion 99:23
5. Kharton VV, Shuangboa L, Kovalevski AV, Naumovich EN (1997) Solid State Ion 96:141
6. Kharton VV, Kovalevsky AV, Viskup AP, Shaula AL, Figueredo FM, Naumovich EN, Marques FMB (2003) Solid State Ion 160:247
7. Li S, Jin W, Xu N, Shi J (1999) Solid State Ion 124:161
8. van Hassel BA, Kawada T, Sakai N, Yokokawa H, Dokiya M, Bouwmeester HJM (1993) Solid State Ion 66:295
9. Katsuki M, Wang S, Dokiya M, Hashimoto T (2003) Solid State Ion 156:453
10. Shao Z, Yang W, Cong Y, Dong H et al (2000) J Membr Sci 172:177
11. Zhu X, Wang H, Yang W (2004) Chem Commun 1130
12. Wang H, Tablet C, Feldhoff A, Caro J (2005) Adv Mater 17:1785
13. Nakamura T, Petzow G, Gauckler LJ (1979) Mater Res Bull 14:649
14. Ullmann H, Trofimenko NJ (2001) J Alloys Compd 316:153
15. Ullmann H, Trofimenko N, Tietz F, Stöver D, Ahmad-Khanlou A (2000) Solid State Ion 138:79
16. Teske K, Ullmann H, Trofimenko N (1997) J Therm Anal Calorim 49:1211
17. Mizusaki J, Mima Y, Yamauchi S, Fueki K (1989) J Solid State Chem 80:102
18. Mizusaki J, Yoshihiro M, Yamauchi S, Fueki K (1985) J Solid State Chem 58:257
19. Lankhorst MHR, ten Elshof JE (1997) J Solid State Chem 130:302
20. Girdauskaite E, Ullmann H, Vashook VV, Bülow M, Guth U (2006) Solid State Ionics (In press)
21. Trofimenko NE, Ullmann H (2000) J Eur Ceram Soc 20:1241
22. Vashook VV, Zinkevich MV, Zonov YuG (1999) Solid State Ion 116:129